Dynamic Mechanical Properties of Poly(oxypropylenediol) and -triol)

Hery Randrianantoandro and Taco Nicolai*

Laboratoire de Physico Chimie Macromoléculaire, URA CNRS, Université du Maine, 72017 Le Mans Cedex, France

Received July 12, 1996; Revised Manuscript Received September 24, 1996[⊗]

ABSTRACT: Oscillatory shear measurements were done on linear poly(oxypropylenediol) and star-shaped poly(oxypropylenetriol) with three arms of equal length. Internal relaxation modes are observed in addition to the local segmental relaxation (α-relaxation) for all molar masses investigated between 500 and 8000 g/mol. The α-relaxation is well described by a generalized exponential relaxation time distribution in which the parameters have been chosen to give a close correspondence with a stretched exponential decay in the time domain. The corresponding stretched exponent $\beta = 0.49 \pm 0.01$ and is the same for the diol and triol and independent of the molar mass. The temperature dependence of the internal modes is the same for the diol and triol and independent of the molar mass but is weaker than that of the α-relaxation close to the glass transition temperature. The shape of the internal modes' relaxation fits well to the Rouse model, and the molar mass dependence of the slowest relaxation time is stronger than expected from the Rouse model. At a given arm length, taking the linear diol as consisting of two arms, the internal modes of the triol and diol are the same within experimental error. A triol with weight average molar mass 260 g/mol, which corresponds to, on average, less than one POP segment per arm, does not show internal modes and has a significantly broader α-relaxation.

Introduction

Dynamic properties of low molar mass poly(oxypropylenediol) and -triol) (POP diol and triol) have been studied earlier using dielectric relaxation,[1−5] shear compliance,[6−8] and light scattering measurements.[9,10] Both local segmental relaxation (the so-called α-relaxation) and large scale chain relaxations have been observed. The latter have been explained in terms of normal modes using the Rouse model, as the molar masses used were lower than the minimum required for entanglements, which is about 7000 g/mol.[11] By these techniques only the one or two slowest normal modes were observed. The molar mass dependence of the relaxation times of the normal modes is stronger than expected from the Rouse model. In addition, the two relaxation processes do not have the same temperature dependence. Nuclear magnetic resonance measurements show that the molar mass dependence of the self-diffusion is also stronger than expected from the Rouse model.[12] These features have been attributed to the influence of hydrogen bonding, and an attempt has been made to explain them in terms of the coupling model introduced by Ngai and co-workers.[13]

Here we present a study of the shear modulus of POP triol with molar masses between 250 and 8000 g/mol and POP diol with molar masses between 400 and 5000 g/mol. The shear modulus is sensitive to all the normal modes, and except for the smallest triol, both the α-relaxation and a broad spectrum of normal modes are observed. The experimental results are compared with results from dielectric spectroscopy and the predictions of the coupling model.

An ulterior motive of this study is that POP triol is the building unit of polyurethane gels on which we are currently conducting a systematic investigation using a number of different techniques.[14,15]

Experimental Section

POP diols and triols with different molar masses were purchased from Aldrich, and the triols with nominal masses of 720 (T720) and 2500 g/mol were from Arcol. The triols are propylene oxide adducts of trimethylolpropane. The samples were dried under vacuum and characterized using size exclusion chromatography. The polydispersity of all samples characterized by the ratio of the weight average molar mass (M_w) to the number average molar mass (M_n) is less than 1.05. The samples T6000 and D4000 contain a lower molar mass fraction of about 15%, while the samples T4100 and D3000 contain a lower molar mass fraction of about 5%. Taking into account the lower molar mass fractions increases, of course, the polydispersity of these samples. For the low molar mass samples (M < 1000 g/mol) the individual oligomers can be distinguished and weight average molar masses can be established accurately. The molar mass of the larger fractions has been calculated from the measured hydroxyl content by assuming complete functionality. This procedure does not lead to the true molar mass for the samples which contain a low molar mass fraction with probably a different functionality. The molar mass of these samples has been determined by light scattering with an uncertainty of 10−20%.

The weight average molar masses are summarized in Table 1. We also give the weight average number of POP segments for each sample.

Calorimetric glass transition temperatures, T_{gc}, were measured using differential scanning calorimetry. The samples were cooled rapidly to 100 K and then heated at a rate of 10 deg/min. Values of T_{gc} taken as the midpoint of the transition are given for each sample in Table 1. The reproducibility is ±2 deg.

Dynamic shear measurements were done on a Rheometrics RDA II dynamic spectrometer using parallel-plate geometry at temperatures between 200 and 340 K. In the so-called hold mode, the gap is corrected for temperature variations of the sample volume. The plate size (diameter between 50 and 4 mm) and the imposed deformation (0.2−20%) were adjusted to obtain an accurate torque response while remaining in the linear regime. The shear modulus could be measured in the range $10-10^9$ Pa. We were able to measure very large moduli by using a relatively large sample thickness (2−2.5 mm) in combination with a small plate size.

Results

We will treat the smallest triol (T260) as a special case and discuss first the results of the other systems. Master curves of the loss (G'') and storage (G')

[⊗] Abstract published in *Advance ACS Abstracts,* April 1, 1997.

S0024-9297(96)01016-9 CCC: $14.00

Table 1. Sample Characteristics

sample	M_w (kg/mol)	T_{gv} (K)	T_{gc} (K)	N
D425	0.43	197.5	208	5.6
D2000	2.1	202.5	211	34.5
D3000	3.7	202.5	213	62
D4000	4.8	202.5	212	81
T260	0.26	218.5	227	2.2
T720	0.73	212.5	219	10.2
T2500	2.8	207.5	213	46
T4100	4.8	204.5	214	80
T6000	7.7	203.5	213	130

moduli were obtained by time−temperature superposition. Figure 1 shows the data for the smallest and largest diol and triol on a semilogarithmic scale. In such a representation essentially only the α-relaxation is visible. To facilitate the comparison of the shape of the α-relaxation, the master curves are normalized by the maximum of the loss modulus (G''_{max}) and plotted as a function of ω/ω_{max}, where ω_{max} is the position of G''_{max}. G''_{max} is, within the experimental error, the same for all samples: $(1.4 \pm 0.15) \times 10^8$ Pa. It is clear that the shape of the α-relaxation is independent of the molar mass and is the same for diol and triol. The identical shape of the α-relaxation together with the very weak variation in the glass transition temperature implies that the effects of end groups and the central core on the glass transition dynamics are very small.

We have fitted the data using a generalized exponential relaxation time distribution ($A_g(\tau)$), as described in ref 16:

$$G'(\omega) = G_0 \int_0^\infty A_g(\tau) \frac{\omega^2\tau^2}{1+\omega^2\tau^2}\, d\tau$$
$$G''(\omega) = G_0 \int_0^\infty A_g(\tau) \frac{\omega\tau}{1+\omega^2\tau^2}\, d\tau \qquad (1)$$

with

$$A(\tau) = \frac{K|s|\tau_g^{-p}\tau^{p-1}\exp[-(\tau/\tau_g)^s]}{\Gamma\left(\frac{p}{s}\right)}$$

where K is a normalization constant such that $\int_0^\infty A(\tau)\, d\tau = 1$, τ_g is a characteristic relaxation time, and p and s are parameters which determine the shape of the distribution. This function is equivalent to other empirical functions, such as the Williams−Watts or the Havriliak−Negami functions, but allows one to fit easily in both the time and the frequency domain. Equation 1 is equivalent to a stretched exponential decay in the time domain: $G(t) = G_0 \exp[-(t/\tau_s)^\beta]$ for $\beta < 0.6$ if we chose $p = s/(s-1) = \beta$ (see ref 16). The best agreement with the data was obtained with $\beta = 0.49$ (see solid lines in Figure 1), which is close to the value obtained by dielectric spectroscopy and depolarized dynamic light scattering measurements on POP diol. G_0 is, within the experimental error, the same for all samples: $(5.5 \pm 0.5) \times 10^8$ Pa.

As can be observed in a double logarithmic representation (see Figure 2), at lower frequencies the α-relaxation crosses over into another relaxation process, which we attribute to the relaxation of internal modes. The width of the slower relaxation process decreases with decreasing molar mass but is visible even for the samples D425 and T720, which contain only a few POP

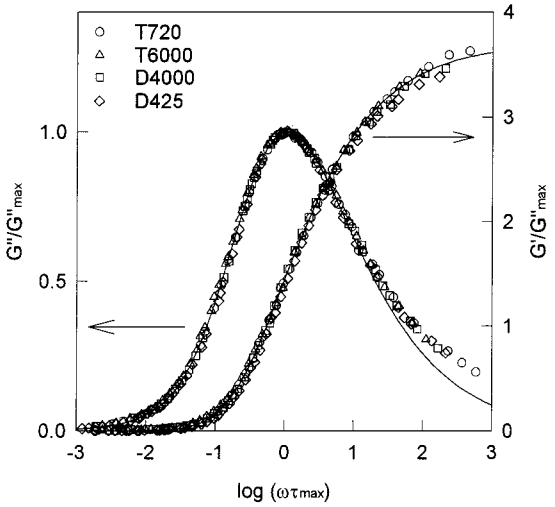

Figure 1. Semilogarithmic representation of the frequency dependence of the normalized storage and loss shear modulus of the POP diol and triol samples indicated in the figure.

segments. It is clear that this second relaxation process has a slightly weaker temperature dependence so that time−temperature superposition does not give a unique master curve.

The temperature dependence of ω_{max} is shown in Figure 3. The reference temperature (T_{ref}) is the temperature where $\omega_{max} = 1$ rad/s, which can be considered as the viscoelastic glass transition temperature (T_{gv}). The values of T_{gv} are about 10 deg below the calorimetric values and are summarized in Table 1. For T720 and D425 the α-relaxation dominates the signal, especially G'', so that the shift factors for these samples are essentially those of the α-relaxation even at frequencies far below ω_{max}. For the larger molar masses we can obtain the temperature dependence of the α-relaxation only over a small temperature range because at higher temperatures we can solely measure the internal modes relaxation. Within experimental error the temperature dependence is independent of the molar mass and is well described by the so-called Vogel−Fulcher (VF) equation:

$$\log(\omega_{max}) = 13.2 - \frac{466}{(T - T_{gv}) + 35} \qquad (2)$$

For comparison, we have included results from dielectric measurements reported in refs 1 and 5. In these measurements on linear POP no molar mass dependence was detected and we have used $T_{gv} = 202.5$ K in the comparison, which is the temperature where $\omega_{max} = 1$ rad/s.

To study the relaxation of internal modes, we did a time−temperature superposition of the slower process after a vertical shift T_{ref}/T to correct for the temperature variation of the strength of the internal modes relaxation. Due to the limited dynamic range of the rheometer, we can observe the two processes together in the experimental window only over a small temperature range. The resulting master curves for D4000 are shown in Figure 4. Deviations at higher frequencies are clearly visible, especially for G'', for which the influence of the α-relaxation extends to lower frequencies. Similar plots are obtained for all samples.

In order to describe the data quantitatively, we have assumed that the slow relaxation can be described by a sum of so-called Rouse normal modes. For regular star-branched polymers with f arms of length L, taking linear chains as stars with two arms, the relaxation time of

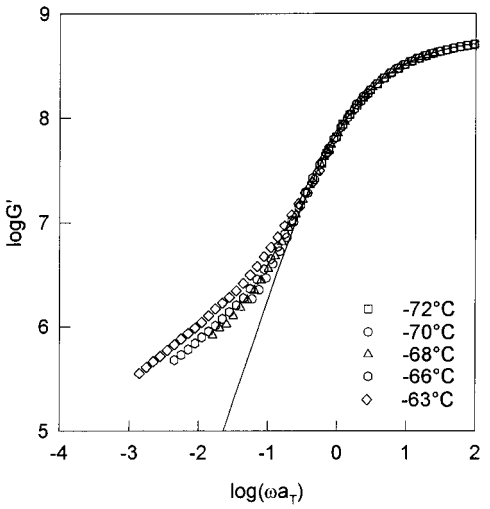

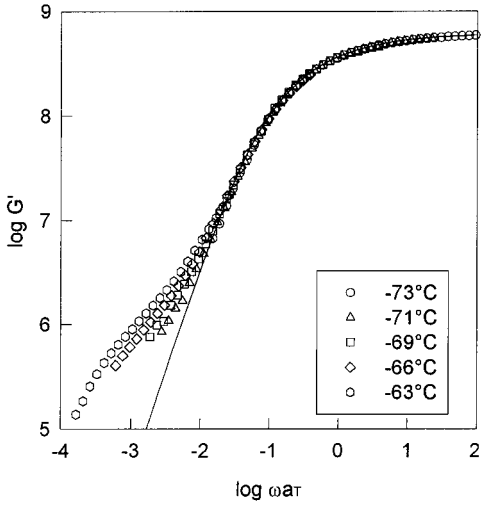

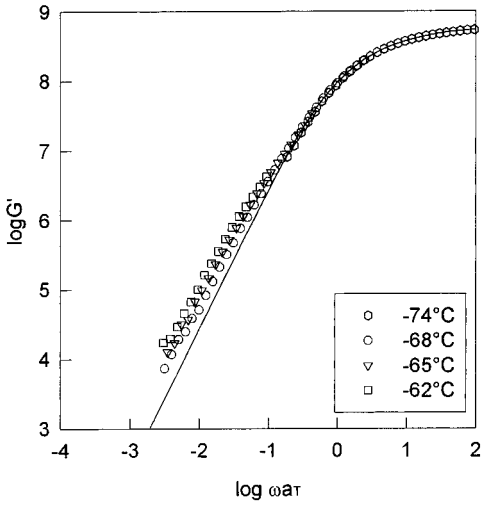

Figure 2. Double logarithmic representation of the frequency dependence of the normalized storage shear modulus of the samples D4000 (top), D2000 (middle), and D425 (bottom). The curves were obtained using time−temperature superposition at high frequencies. The reference temperatures are 203, 205, and 202 K, respectively.

the pth Rouse mode is given by[17,18]

$$\tau_p = \frac{L^2\xi}{3\nu^2 \sin^2[p\pi/2(\nu+1)]kT} \tag{3}$$

where k is the Boltzmann constant, ν is the total number of modes, and ξ is a friction coefficient. The shear moduli are given by the sum of the Rouse modes and the generalized exponential (GEX) relaxation time distribution, which describes the α-relaxation:

$$G' = C_r \sum_{p=1}^{\nu} h \frac{\omega^2\left(\frac{1}{2}\tau_p\right)^2}{1+\omega^2\left(\frac{1}{2}\tau_p\right)^2} + C_g\int_0^\infty A_g(\tau)\frac{\omega^2\tau^2}{1+\omega^2\tau^2}\,d\tau$$

$$G'' = C_r \sum_{p=1}^{\nu} h \frac{\omega\left(\frac{1}{2}\tau_p\right)}{1+\omega^2\left(\frac{1}{2}\tau_p\right)^2} + C_g\int_0^\infty A_g(\tau)\frac{\omega\tau}{1+\omega\tau}\,d\tau \tag{4}$$

Here C_r and C_g are the amplitudes of the Rouse modes and the α-relaxation, respectively. The prefactor h is introduced to take into account that the amplitude of the odd modes increases with increasing number of arms: $h = 1$ for even modes and $h = f - 1$ for odd modes. The amplitude of the Rouse modes is given by $C_r = \rho RT/M$, where R is the gas constant and ρ is the density. In the time−temperature superposition, we have corrected for the temperature dependence of C_r. It is not clear what the temperature dependence of C_g is, but over the small temperature range where the α-relaxation is important, we can neglect this dependence.

The difference between the frequency dependence of the shear modulus using the Rouse spectrum with f equal to 2 or 3 is quite small. This is illustrated in Figure 5 where G'/C_r is plotted versus $\omega\tau_1$ for D4000 and T4100 together with the theoretical predictions for f equal to 2 and 3. In practice, it is impossible to distinguish between a diol and a triol on the basis of the shape of the shear modulus. A fit of a linear chain Rouse spectrum to a triol leads to an overestimation of τ_1 by about 10% and of C_r by about a 50%.

The contribution of the Rouse modes and the α-relaxation to G' and G'' is shown schematically in Figure 6. The effect of a different temperature dependence for

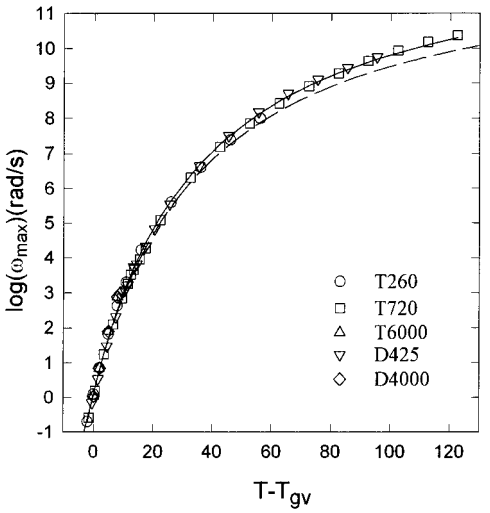

Figure 3. Temperature dependence of ω_{max} obtained from dynamic mechanical measurements for the samples indicated in the figure. The data are plotted as a function of $T - T_{gv}$ with T_{gv} defined as the temperature where $\omega_{max} = 1$ rad/s; see Table 1. The solid line represents eq 2. The dashed line represents the results from dielectric spectroscopy.

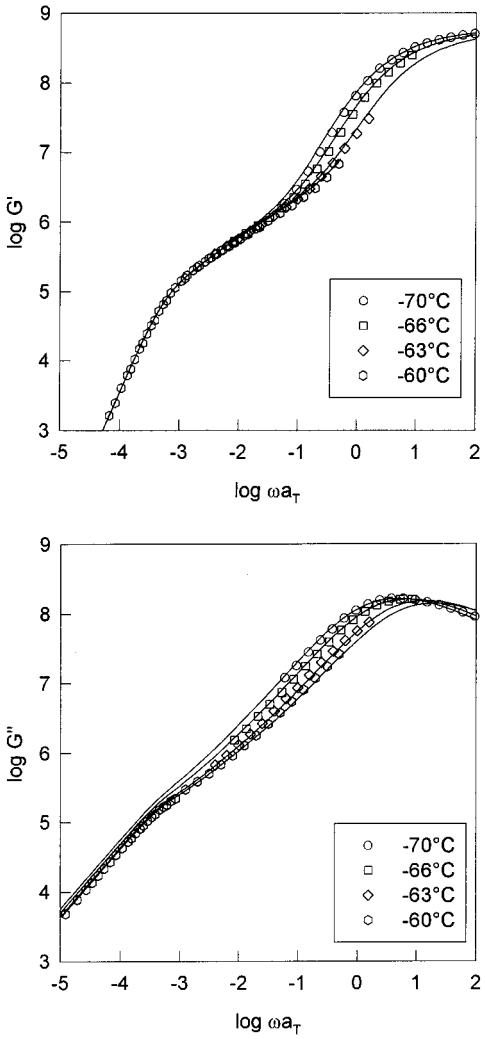

Figure 4. Double logarithmic representation of the frequency dependence of the storage (top) and loss (bottom) shear modulus of the sample D4000 at different temperatures indicated in the figure. The triangles represent temperatures above 214 K. The data at different temperatures were superimposed to overlap at low frequencies. The solid lines represent fits to eq 4.

the two processes is shown in Figure 7, where τ_1 is kept constant at 2×10^4 s and $\tau_{max} = 1/\omega_{max}$ is varied between 0.1 and 10 s. It is clear that when τ_1 and τ_{max} are close, G'' is modified by the α-relaxation even at low frequencies. G' is not modified at low frequencies so that a time−temperature superposition is possible even if τ_1 and τ_{max} are close, provided one uses G'. This is illustrated for D2000 in Figure 8.

The solid lines in Figures 4 and 8 represent fits of the data to eq 4 at different temperatures. The model gives a good description of the data. We note that a continuous distribution of Rouse modes, i.e. $G' \propto G'' \propto \omega^{0.5}$, does not give as good a fit. As mentioned above, C_g is, within the experimental error, the same for all samples: $(5.5 \pm 0.5) \times 10^8$ Pa. The fit is rather insensitive to ν as long as τ_ν is not much larger or smaller than $20\tau_{max}$. We stress, however, that the data cannot be fitted if we use only one or two modes, contrary to what has been observed for dielectric relaxation and shear compliance measurements. The only fit parameters are thus C_r, τ_1, and τ_{max}. The temperature dependence of τ_1 is shown in Figure 9 together with the VF equation for τ_{max} (eq 2). For comparison, we have included results from dielectric

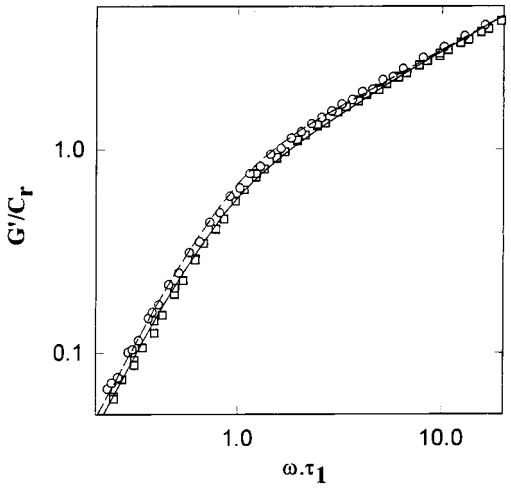

Figure 5. Comparison of the frequency dependence of the storage modulus of D4000 (squares) with that of T4100 (circles). The angular frequency is normalized by the relaxation time of the slowest normal mode and the modulus is normalized by the amplitude of this mode. The solid and dashed lines are fits to eq 4 with f equal to 2 and 3, respectively.

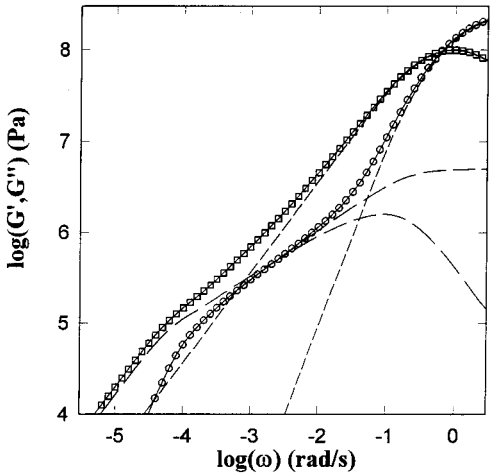

Figure 6. Illustration of the storage (squares) and loss (circles) shear modulus calculated using eq 4. The parameters correspond approximately to those used to fit the data of D4000. The contribution of the Rouse normal modes and the α-relaxation are shown by the long and short dashed lines, respectively.

spectroscopy on two linear POP samples reported in ref 1. From the structure of linear POP it can be argued that dielectric relaxation due to internal modes is dominated by the second normal mode,[3] which has therefore been multiplied by 4 for comparison with τ_1 in Figure 9. Qualitatively, the results of the two techniques are the same, but for a detailed quantitative comparison it is necessary to do measurements on the same samples.

In Figure 9b we have normalized the data at $T - T_{gv} = 70.5$, which is close to 0 °C for the larger diols and triols. It is clear that for all samples the temperature dependence is the same except close to the glass transition temperature where the data show some scatter. Except at very low temperatures, a single VF equation describes well all the data including the dielectric spectroscopy results.

$$\log(a_r) = -4.45 + \frac{489}{(T - T_{gv}) + 39.5}(T - T_{gv})_{ref} = 70.5 \quad (5)$$

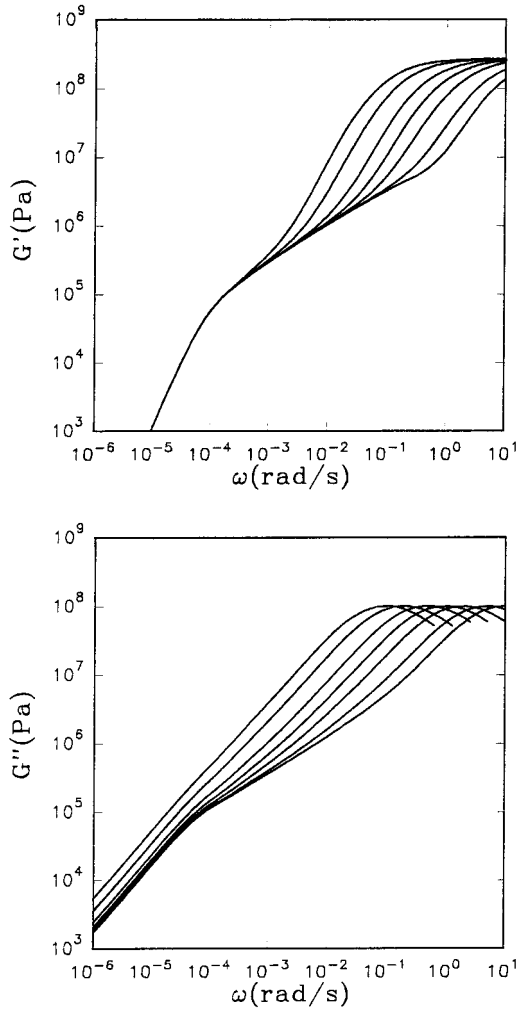

Figure 7. Illustration of the effect on the storage (top) and loss (bottom) shear modulus of a different temperature dependence of the Rouse normal modes and the α-relaxation. The relaxation times of the normal modes are kept constant, while that of the α-relaxation is varied by up to a factor 100.

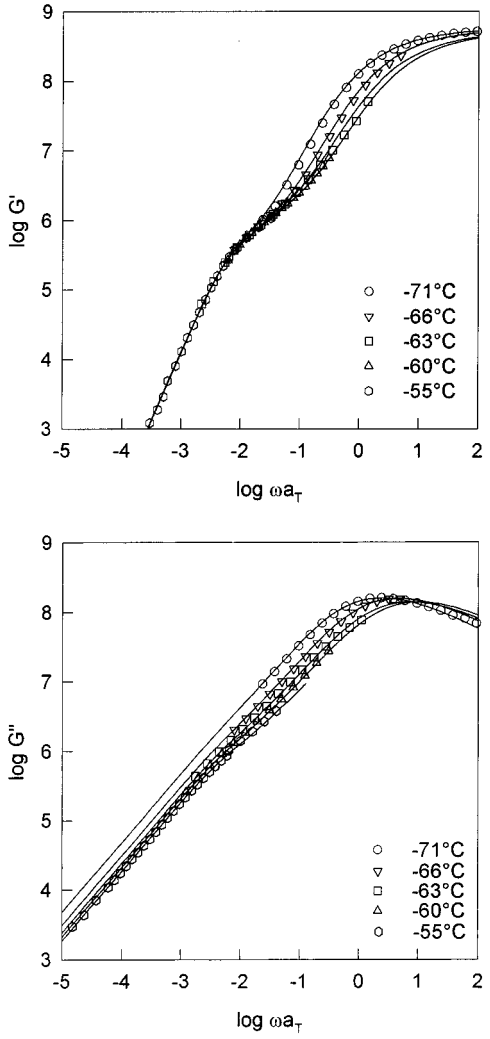

Figure 8. Double logarithmic representation of the frequency dependence of the storage (top) and loss (bottom) shear modulus of the sample D2000. The data at different temperatures were superimposed to overlap at low frequencies for G'. The solid lines represent fits to eq 4.

We also show in Figure 9b the shift factors of the α-relaxation. It is clear that the temperature dependence of the two relaxation processes is very close, except for $T < T_{gv} + 20$, where the α-relaxation has a stronger temperature dependence. We stress, however, that we can measure both modes on the same sample only over a limited temperature range close to T_{gv} and we have assumed that the temperature dependence of τ_{max} at higher temperatures of the larger samples is the same as that of the smaller samples for which it can be measured. This assumption seems justified by the results of dielectric spectroscopy.

The values of τ_1 and C_r at $T - T_{gv} = 70.5$ are summarized in Table 2. For $v > 10$, τ_1 varies only very weakly with v and is given by

$$\tau_1 = \frac{4b^2(N/f)^2\xi}{3\pi^2 kT} \tag{6}$$

where N/f is the number of propylene oxide segments per arm with size b. In Figure 10 the values of τ_1 at $T - T_{gv} = 70.5$ are plotted versus N/f. The values of τ_1 for POP diol and triol are within experimental error the same if the diol and triol have the same number of segments per arm. The molar mass dependence ($\tau_1 \propto N^{3.2}$) is stronger than expected for Rouse modes and is close to the dependence obtained from dielectric measurements.[1]

The viscosity has been calculated from the low-frequency loss modulus using $\eta = G''/\omega$, and is close to the values given in the literature. However, for the smaller samples the contribution of the α-relaxation to the viscosity cannot be neglected. Only results of large samples should be used to compare the molar mass dependence of the viscosity with the prediction from the Rouse model.

The T260 sample has a significantly higher glass transition temperature than the larger triols and diols. It is clear that for this sample, and to a lesser extent the T720 sample, the influence of the core becomes important. SEC shows that the T260 sample is essentially a mixture of two oligomers containing two and three POP segments. The master curves of the shear moduli plotted in Figure 11 show no presence of the internal modes' relaxation. The α-relaxation is broader and is characterized by $\beta = 0.45$. The increase in the width could be due to the fact that the two oligomers in the sample have different glass transition temperatures. The temperature dependence of ω_{max} is included in Figure 10 and is indistinguishable from the other samples.

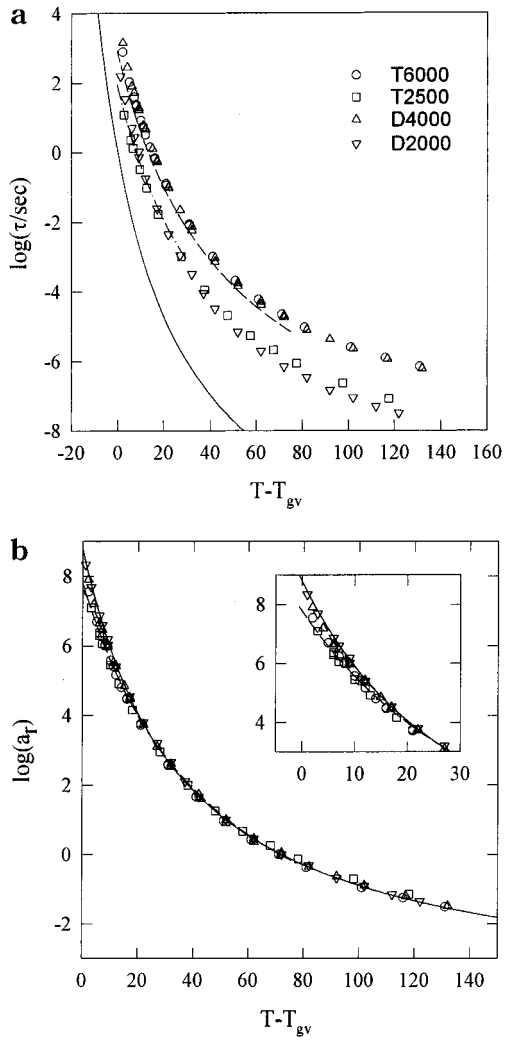

Figure 9. (a) Temperature dependence of τ_1 obtained from dynamic mechanical measurements for the samples indicated in the figure. The data are plotted as a function of $T - T_{gv}$ with T_{gv} defined as the temperature where $\tau_{max} = 1$ s; see Table 1. The solid line represents the α-relaxation. The dashed and dashed-dotted lines represent the results from dielectric spectroscopy for POP diols with nominal masses of 4000 and 2000 g/mol, respectively, taken from ref 1. (b) The same data as in (a) with the relaxation times normalized by the value at $T - T_{gv} = 70.5$. The insert shows a closeup of the data close to $T = T_{gv}$.

Table 2. Values of the Relaxation Times of the First Normal Mode and the Amplitude of Rouse Modes at $T - T_{gv} = 70.5$

sample	τ_1 (μs)	$C_r \times 10^{-5}$ (Pa)
D2000	1.42	5.1
D3000	8.8	2.8
D4000	36	1.8
T2500	1.8	4.2
T4100	8.4	2.5
T6000	40	1.1

Summary and Discussion

The form of the α-relaxation of the shear modulus of POP diol and triol is the same and independent of the molar mass, except for T260, which is somewhat broader. A slower relaxation process is observed even for samples containing only a few POP segments. This relaxation is well described by a sum of Rouse normal modes. It is clear, however, that internal modes characterizing the movement of only a few segments cannot be understood in terms of the Rouse model. We are not aware of the existence of a theory on the crossover between the α-relaxation and the internal modes relaxation that can explain our observations. Close to T_g the temperature dependence of the relaxation times of the internal modes is weaker than that of the α-relaxation, but it is the same for the diol and triol and independent of the molar mass. The molar mass dependence of the relaxation times of the internal modes at a given temperature is stronger than expected. For a given arm length, the relaxation times of the internal modes of the triol and diol are the same within experimental error.

It has often been assumed in the past that the friction coefficient which controls the internal modes has the same temperature dependence as that which controls the α-relaxation. In this case, time−temperature superposition is possible over the whole frequency range. However, different temperature dependences for the shift factors of the α-relaxation (a_1) and the internal modes (a_2) have been reported for POP diol and several other polymers.[1,2,6,19−24] The difference has been interpreted in terms of a mode coupling theory as being due to a stronger coupling of the segmental relaxation to its environment. This would lead to a stronger increase of τ_{max} than of τ_1 with decreasing temperature. Alternatively, one can view the different temperature dependence as a decoupling of the two relaxation modes close

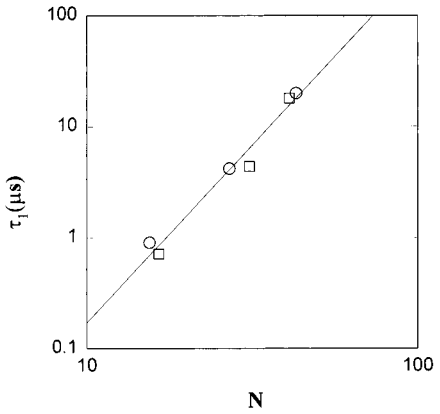

Figure 10. Double logarithmic representation of the relaxation time of the slowest normal mode as a function of the number of propylene oxide segments per arm of POP triol (circles) and diol (squares). The solid line represents a linear least squares fit to all the data and has slope 3.2.

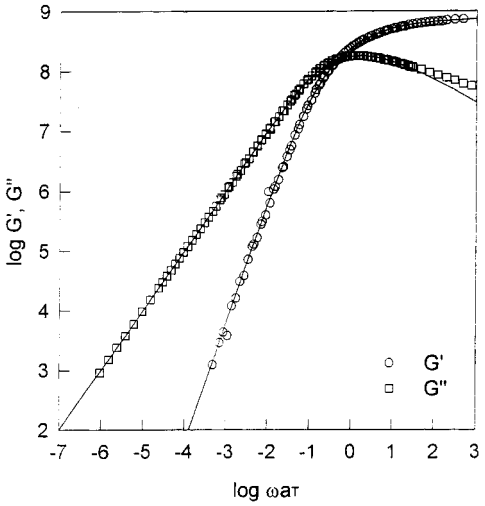

Figure 11. Double logarithmic representation of the frequency dependence of the normalized storage and loss shear modulus of the sample T260. The curves were obtained using time−temperature superposition.

to T_g. Both interpretations have been given to the same set of dielectric results on POP diol.[2,13]

One of the predictions of the mode coupling model is that $\log(a_1) = (\beta_2/\beta_1) \log(a_2)$, where β_1 and β_2 are the exponents of the stretched exponentials that characterize the width of the α-relaxation and each internal mode relaxation, respectively. Over the limited temperature range where we can measure both modes, the logarithm of the shift factors is approximately proportional, with a proportionality factor of 1.2, which is somewhat smaller than the value 1.38 obtained from dielectric spectroscopy for POP diol.[13] These results imply that $\beta_2 < 1$ and that the internal modes' relaxation is characterized by a series of stretched exponential decays instead of simple exponential decays, as assumed above. The deviation from single exponential decays has been attributed to coupling of the normal modes to their environment through hydrogen bonding. It is clear, however, both from the dielectric measurements and from our mechanical measurements that the discrepency disappears at high temperatures, which is not predicted by the mode coupling model. A decoupling of the two processes close to T_g seems a more appropriate model.

The stronger than expected molar mass dependence of the relaxation times of the normal modes is also explained by the coupling model in terms of coupling of the normal modes to their environment: $\tau_p \propto M^{2/\beta_2}$. However, even if we accept a stretched exponential decay of the internal modes, the molar mass dependence of τ_p and the ratio $\log(a_1(T))/\log(a_2(T))$ do not lead to the same values of β_2.

References and Notes

(1) Schönhals, A.; Schlosser, E. *Phys. Scr.* **1993**, *T49*, 233.
(2) Schlosser, E.; Schönhals, A. *Prog. Colloid Polym. Sci.* **1993**, *91*, 158.
(3) Bauer, M. E.; Stockmayer, W. H. *J. Chem. Phys.* **1965**, *43*, 4319.
(4) Stockmayer, W. H.; Bauer, M. E. *Macromolecules* **1969**, *2*, 647.
(5) Yano, S.; Rabalkar, R. R.; Hunter, S. P.; Wang, C. H.; Boyd, R. H. *J. Polym. Sci., Polym. Phys. Ed.* **1976**, *14*, 1877.
(6) Cochrane, J.; Harrison, G.; Lamb, J.; Phillips, D. W. *Polymer* **1980**, *21*, 837.
(7) Alper, T.; Barlow, A. J.; Gray, R. W. *Polymer* **1976**, *17*, 665.
(8) Barlow, A. J.; Erginsav, A. *Polymer* **1975**, *16*, 110.
(9) Wang, C. H.; Fytas, G.; Lilge, D.; Dorfmüller, Th. *Macromolecules* **1981**, *16*, 1363.
(10) Duggai, A. R.; Nelson, K. A. *J. Chem. Phys.* **1991**, *12*, 7677.
(11) Smith, B. A.; Samulski, E. T.; Yu, L.-P.; Winnik, M. A. *Phys. Rev. Lett.* **1984**, *52*, 45.
(12) Cosgrove, T.; Griffiths, P. C.; Webster, J. R. P. *Polymer* **1994**, *35*, 140.
(13) Ngai, K. L.; Schönhals, A.; Schlosser, E. *Macromolecules* **1992**, *25*, 4915.
(14) Tabellout, M.; Baillif, P. Y.; Randrianantoandro, H.; Litzinger, F.; Emery, J. R.; Nicolai, T.; Durand, D. *Phys. Rev. B* **1995**, *51*, 12295.
(15) Randrianantoandro, H.; Nicolai, T.; Durand, D.; Prochazka F. *J. Non-Newtonian Fluid Mech.* **1996**, *77*, 311.
(16) Nicolai, T.; Gimel, J. C.; Johnsen, R. *J. Phys. II* **1996**, *6*, 697.
(17) Ferry, J. D. *Viscoelastic properties of polymers*, 3rd ed.; Wiley: New York, 1980. Strobl, G. *The Physics of Polymers*; Springer-Verlag: Berlin, 1996.
(18) Ham, S. J. *J. Chem. Phys.* **1957**, *26*, 625.
(19) Ngai, K. L.; Plazek, D. J.; Deo, S. S. *Macromolecules* **1987**, *20*, 3047.
(20) Plazek, D. J.; Zheng, X. D.; Ngai, K. L. *Macromolecules* **1992**, *25*, 4920.
(21) Plazek, D. J.; Schlosser, E.; Schönhals, A.; Ngai, K. L. *J. Chem. Phys.* **1993**, *8*, 6488.
(22) Fytas, G.; Dorfmüller, T.; Chu, B. *J. Polym. Sci.* **1984**, *22*, 1471.
(23) Schönhals, A. *Macromolecules* **1993**, *26*, 1309.
(24) Palade, L. I.; Verney, V.; Attané, P. *Macromolecules* **1995**, *28*, 7051.

MA9610166